Central European Journal of Energetic Materials, **2014**, *11*(1), 157-170
ISSN 1733-7178

Initiation Capacity of a New Booster Pellet

Lishuang HU*, Shuangqi HU and Xiong CAO

Chemical Industry and Ecology College, North University of China, Taiyuan, Shanxi 030051, P.R. China
**E-mail: hlsly1314@163.com*

Abstract: Insensitive munitions improve the survivability of both weapons and their associated platforms. All weapon systems contain an explosive train which needs to meet the insensitive munitions criteria but also to reliably initiate the main charge explosive. The traditional cylindrical booster pellet has insufficient energy output to reliably initiate an insensitive main charge explosive. To ensure that this requirement can be achieved, a new highly effective booster charge structure was designed. New booster pellets of four different sizes were investigated by numerical simulation and the one with the most powerful output was selected for experimental study. The results show that the new booster pellet has more initiation capacity than a cylindrical booster pellet with the same mass and pressed density. The convergence pressure of the new booster pellet is much higher than that of a cylindrical booster pellet with the same density.

Keywords: explosion mechanics, booster pellet, main charge, initiation capacity

1 Introduction

The recent focus on insensitive munitions (IM) has directed research towards ingredients and formulations that can be used to produce insensitive explosives and ordnance, with efforts largely concentrated on the main charge filling. Another key component of any munition is the booster system, which is required to reliably initiate the main charge. The exploitation of IM technology leads to improved survivability, from accident or enemy action, of both the weapon systems and their associated platforms [1]. In addition, their use results in reduced casualties, reduced mission losses and whole life costs, while still supplying an

equivalent performance.

Both complex and general munitions contain a number of explosive trains to provide reliable initiation and detonation transfer. As the main charge fillings for weapons are becoming increasingly insensitive to hazard threat stimuli, the traditional method of increasing the energy output to reliably initiate the insensitive main charge explosive is to increase the size and amount of the booster explosive [2]. This has resulted in the explosive train becoming a significant factor in overall weapon vulnerability.

Developments on booster explosives have therefore been aimed at new, highly effective booster charge structures of small size and amount that will reliably initiate main charge explosives.

Spahn [3] studied an embedded can booster. A plate was embedded in the main charge explosive and provided a high impedance surface which was shaped and oriented so that shock waves from the booster pellet struck the high impedance surface at normal incidence and were reflected back towards the booster pellet. This increased the pressure in the main charge explosive material between the booster pellet and the plate, thus increasing the effectiveness of the booster pellet. Spahn [4] also studied a booster explosive ring. This explosive device had a main charge explosive and a booster explosive ring with the main charge filling the space in the center of the booster ring. When the booster pellet was initiated, the shock wave converged in the space in the center of the booster pellet, thus initiating the main charge explosive. Dallman [5] studied the initiation technology of a hemispherical booster explosive. The results showed that the output of a hemispherical booster explosive was large for a small size. In our recent work [6], we studied the initiation capacity of a conical ring booster pellet with a multi-point-synchronous explosive circuit. The energy output of the conical ring booster pellet was good, but it had to be initiated by a multi-point synchronous circuit. The explosive charge of the multi-point synchronous circuit was very demanding. If the density of the explosive charge was discontinuous, the synchronous initiation deviation was large, and the initiation capacity of the conical ring booster pellet was greatly affected. Consequently we have designed a new booster pellet having high initiation capacity that could be initiated by a simple method, such as a single-point initiation. The new booster pellets with four different sizes were investigated by numerical simulation and the one with the most powerful output was selected for experimental study.

2 Numerical Simulation

ANSYS/LS-DYNA software using the LS-DYNA explicit finite element program was used. The size and shape of the new booster pellets are shown in Figure 1. The calculation models of the booster pellets are shown in Figure 2.

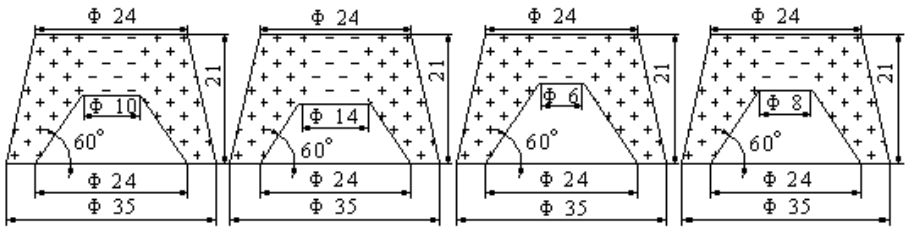

(a) (b) (c) (d)

Figure 1. The shapes and dimensions of the new booster pellets.

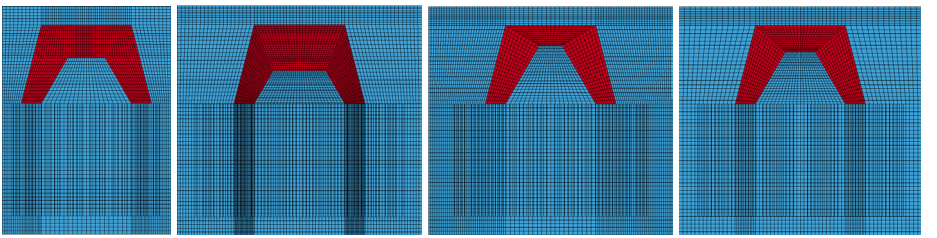

(a) (b) (c) (d)

Figure 2. The finite mesh models.

2.1 Calculation model and element algorithm

The quarter-symmetry model was adopted to establish the finite element model with midpoint initiation on the top. The ALE algorithm was adopted for the charge and air, whereas the Lagrange algorithm was adopted for the steel witness plate. The solid-fluid interaction algorithm was used for the charge, air, and steel witness plate.

2.2 Material models

The pressure in the detonation products from PBXN-5 explosive was characterized with the Jones-Wilkins-Lee (JWL) equation of state [7]. The pressure in either phase is defined in terms of the volume and internal energy as:

$$p = A\left(1-\frac{\omega}{R_1V}\right)e^{-R_1V} + B\left(1-\frac{\omega}{R_2V}\right)e^{-R_2V} + \frac{\omega E}{V} \tag{1}$$

where A, B, R_1, R_2, and ω are adjustable parameters. V is the ratio of the volume of the product gases to the initial volume of the undetonated explosive. E is the specific internal energy.

The air was modelled to represent the medium in which the blast wave propagates. The linear-polynomial equation of state [8] was used to simulate the proper air behaviour:

$$P = C_0 + C_1\mu + C_2\mu^2 + C_3\mu^3 + (C_4 + C_5\mu + C_6\mu^2)E \tag{2}$$

where, $\mu = \rho/\rho_0 - 1$, and ρ/ρ_0 is the ratio of the current density to the initial density, and C_0, C_1, C_2, C_3, C_4, C_5 and C_6 are constants. For gases for which the gamma law equation of state applies such as air, C_0=C_1=C_2=C_3=C_6=0, and C_4=C_5=γ-1, with γ the ratio of specific heats. Therefore, for air, Eq. (2) reduces to:

$$P = (\gamma - 1)\frac{\rho}{\rho_0}E \tag{3}$$

The steel witness plate was 1045 steel. The Johnson-Cook model [9] that accounts for the effects of strain hardening and strain-rate hardening, and the Gruneisen equation of state [10], were adopted to describe the dynamic response of the steel. The Gruneisen equation of state defines pressure for compressed materials as:

$$p = \frac{\rho_0 C^2\mu[1+(1-\frac{\gamma_0}{2})\mu - \frac{a}{2}\mu^2]}{[1-(S_1-1)\mu - S_2\frac{\mu^2}{\mu+1} - S_3\frac{\mu^3}{(\mu+1)^2}]^2} + (\gamma_0 + a\mu)E \tag{4}$$

and for expanded materials as:

$$p = \rho_0 C^2\mu + (\gamma_0 + a\mu)E \tag{5}$$

where C is the intercept of the v_s-v_p curve. S_1, S_2, and S_3 are the coefficients of the slope of the v_s-v_p curve; γ_0 is the Gruneisen gamma; a is the first order volume correction to γ_0; $\mu = \rho/\rho_0 - 1$.

2.3 Numerical simulation results and discussion

(1) Results of booster pellet (a)

The results for booster pellet (a) are shown in Figure 3.

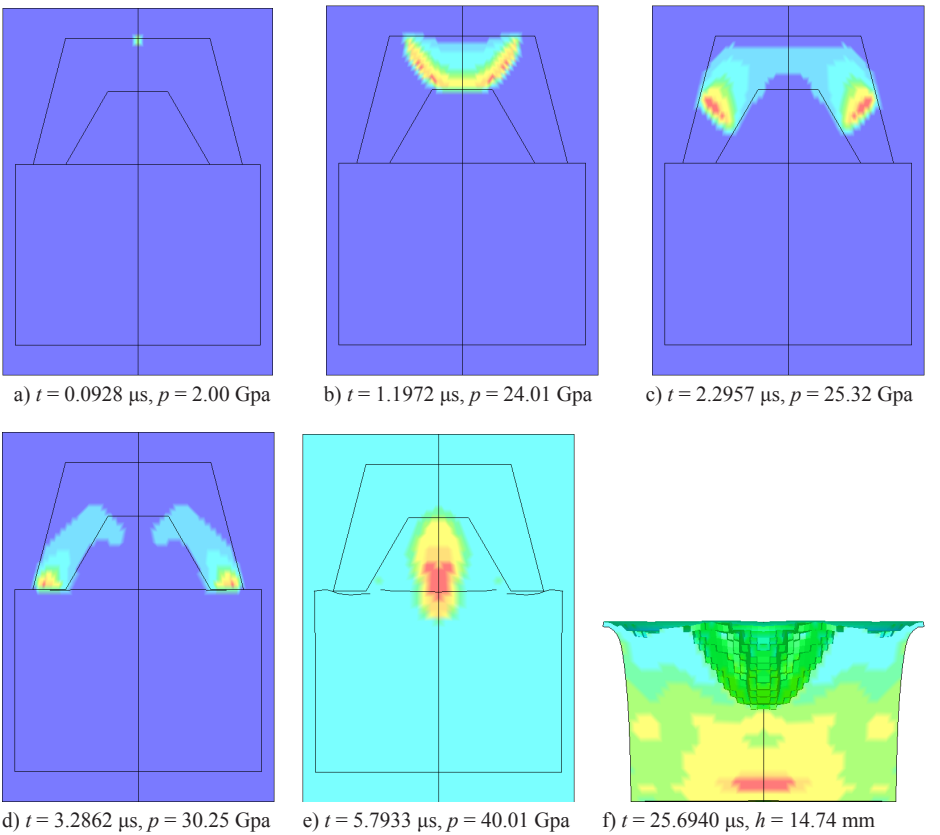

a) t = 0.0928 μs, p = 2.00 Gpa b) t = 1.1972 μs, p = 24.01 Gpa c) t = 2.2957 μs, p = 25.32 Gpa

d) t = 3.2862 μs, p = 30.25 Gpa e) t = 5.7933 μs, p = 40.01 Gpa f) t = 25.6940 μs, h = 14.74 mm

Figure 3. Initiation process of booster pellet (a).

When booster pellet (a) is initiated in the center, the detonation wave propagates downwards in the form of a spherical wave. The detonation pressure significantly increases before the detonation wave reaches the surface of the energy cavity. The peak pressure is 24.01 GPa when t = 1.1972 μs. When the detonation wave reaches the energy cavity surface, the detonation pressure slowly increases due to the impact of rarefaction waves and the thickness of the booster pellet. When t = 3.2862 μs, the detonation waves reach the surface of the steel witness plate, the shockwaves begin to converge towards the energy cavity center, the peak pressure is 30.25 GPa. When t = 5.7933 μs, the convergence pressure reaches its

maximum value of 40.01 GPa. The process of shockwave penetration into the steel witness plate terminates at $t = 25.6940$ μs. The steel dent is 14.74 mm deep.

(2) Results for booster pellet (b)

The results for booster pellet (b) are shown in Figure 4.

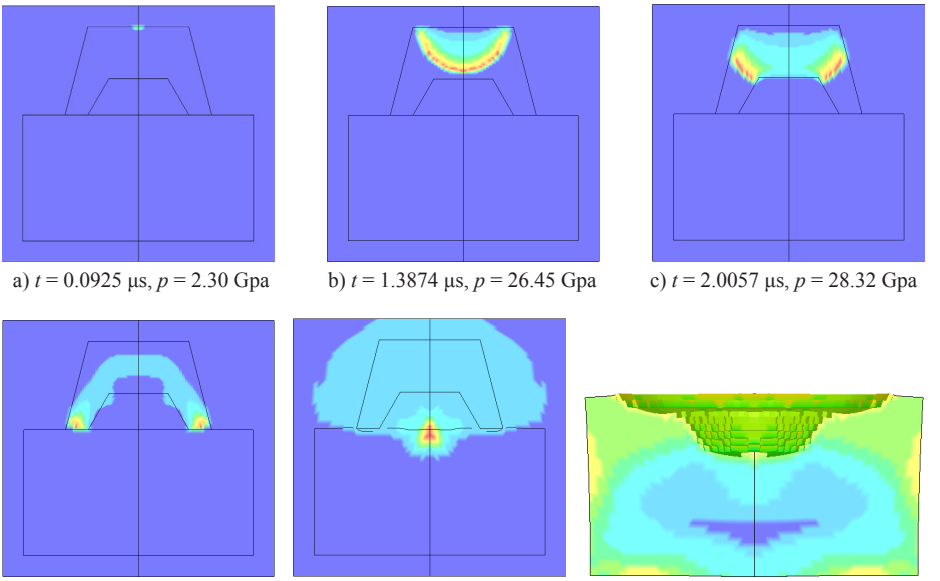

a) $t = 0.0925$ μs, $p = 2.30$ Gpa b) $t = 1.3874$ μs, $p = 26.45$ Gpa c) $t = 2.0057$ μs, $p = 28.32$ Gpa

d) $t = 3.1955$ μs, $p = 29.01$ Gpa e) $t = 5.4234$ μs, $p = 33.21$ Gpa f) $t = 25.0210$ μs, $h = 11.83$ mm

Figure 4. Initiation process of booster pellet (b).

The initiation process of booster pellet (b) is similar to that of booster pellet (a). However, the peak pressure is 33.21 Gpa and the dent depth is 11.83 mm.

(3) Results for booster pellet (c)

The results for booster pellet (c) are shown in Figure 5.

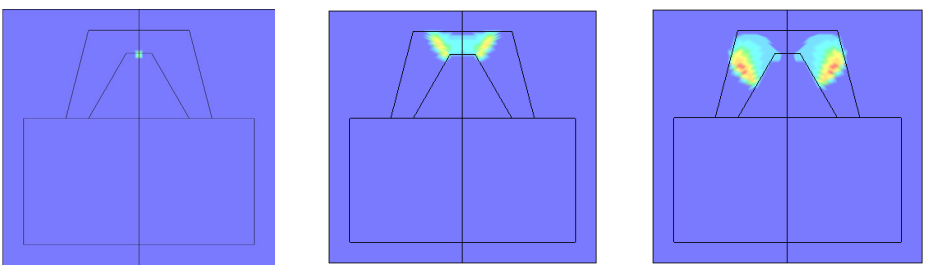

a) $t = 0.0911$ μs, $p = 2.32$ Gpa b) $t = 1.1734$ μs, $p = 21.82$ Gpa c) $t = 2.3582$ μs, $p = 25.22$ Gpa

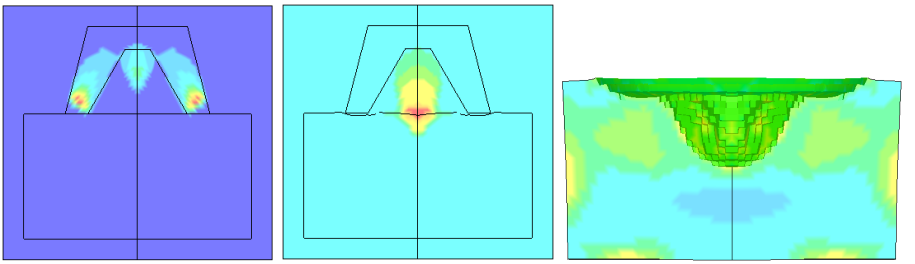

d) t = 3.0916 μs, p = 29.98 Gpa e) t = 5.9312 μs, p = 35.11 Gpa f) t = 25.6875 μs, h = 12.43 mm

Figure 5. Initiation process of booster pellet (c).

The initiation process of booster pellet (c) is similar to that of booster pellet (a). However, the peak pressure is 35.01 Gpa and the dent depth is 12.43 mm.

(4) Results for booster pellet (d)

The results for booster pellet (d) are shown in Figure 6.

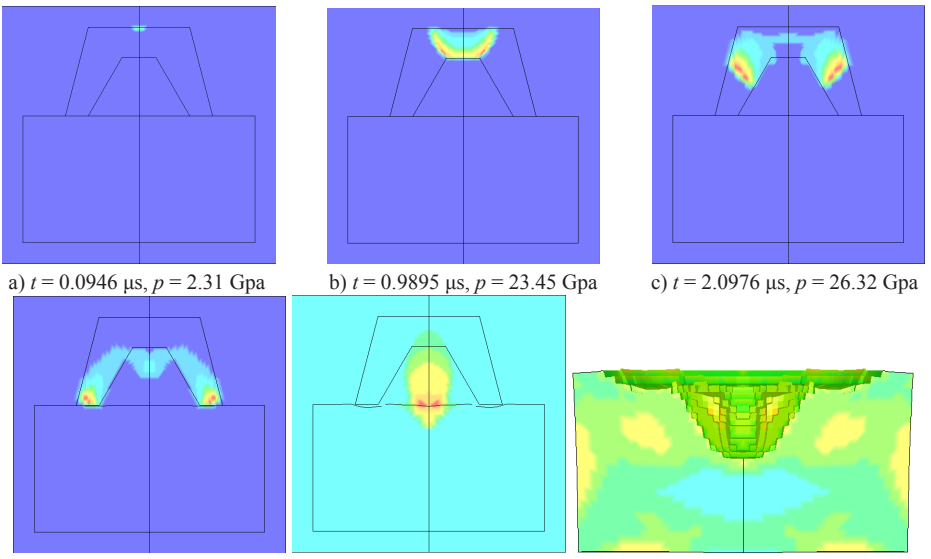

a) t = 0.0946 μs, p = 2.31 Gpa b) t = 0.9895 μs, p = 23.45 Gpa c) t = 2.0976 μs, p = 26.32 Gpa

d) t = 3.2946 μs, p = 30.21 Gpa e) t = 5.8954 μs, p = 37.88 Gpa f) t = 25.7894 μs, h = 13.53 mm

Figure 6. Initiation process of booster pellet (d).

The initiation process of booster pellet (d) is similar to that of booster pellet (a). However, the peak pressure is 37.88 Gpa and the dent depth is 13.53 mm.

Foan and Coley [11] gave an equation to elaborate the shock initiation energy of an explosive. The shock initiation energy E is expressed as:

$$E = \frac{1}{Z}\int_0^{\infty} p^2(t)dt \tag{6}$$

where Z is the shock impedance of the acceptor explosive, $p(t)$ is the shock pressure between the initiation explosive and the acceptor explosive, and t is the action time.

The Eq. (6) is the total energy received by the acceptor explosive from the initiation explosive, but for shock initiation of an explosive, some energy is not used for explosive initiation. Consequently the shock initiation energy E is modified as:

$$E = \frac{1}{Z}\int_0^{t_c} p^2(t)dt \tag{7}$$

where t_c is the time in which the shock pulse decays to p_c, and p_c is the critical initiation pressure.

We wrote a computer program for data processing. Firstly, the data for pressure and time were fitted by the least square method. Then, the shock initiation energy E was calculated using the Simpson integration method. Assuming that the acceptor explosive is TNT, the density is 1.51 g/cm^3, the detonation velocity is 6.8 mm/μs, and the critical initiation pressure is 5.0 Gpa. Thus according to Eq. (7), the shock initiation energies of booster pellets are (a) 28.2, (b) 22.4, (c) 25.1 and (d) 26.4 J/mm^2.

The simulation results and calculation results are shown in Table 1.

Table 1. Simulation results and calculation results

Booster pellet	Simulation maximum pressure (Gpa)	Simulation dent depth (mm)	Shock initiation energy (J/mm^2)
(a)	40.01	14.74	28.2
(b)	33.21	11.83	22.4
(c)	35.11	12.43	25.1
(d)	37.88	13.53	26.4

The simulation results and calculation results show that the initiation capacity of booster pellet (a) is the best. The calculation results are in good agreement with the simulation results.

3 Experimental

In this section we selected the new booster pellet (a) for experimental study on the basis of the numerical simulation and calculation results.

3.1 Experimental method

Four methods are used in this paper [12]. The methods are: (1) the main charge varied-composition method, (2) the main charge axial-steel-dent method, (3) the booster pellet axial-steel-dent method, and (4) the pressure test method. The first two methods have been described in reference [6]. In the booster pellet axial-steel-dent method, the booster pellet is in direct contact with the steel witness plate. Initiated by the detonator, the booster pellet is detonated and produces a dent in the steel witness plate. The depth of the dent is indicative of the booster initiation capacity. In the pressure test method, manganin piezoresistors are used to measure the convergence pressure.

In these experiments, a low resistance manganin piezoresistive sensor was used to measure the convergence pressure more accurately. The pressure can be calculated by the following formula:

$$p = \begin{cases} 53.22\dfrac{\Delta R}{R} & (0 \sim 5.907 \quad Gpa) \\ 1.978 + 35.28\dfrac{\Delta R}{R} & (>5.907 \quad Gpa) \end{cases} \tag{8}$$

In the experiment we adopted a constant current source to measure $\Delta U/U$ by oscillography, and then $\Delta R/R$ was obtained according to the following relationship:

$$\frac{\Delta R}{R} = \frac{\Delta RI}{RI} = \frac{\Delta U}{U} \tag{9}$$

3.2 Experimental conditions

(1) Selection of the booster explosive

The booster explosive PBXN-5 was used in the experiments. The pressed-explosive density of the new booster pellet was 1.68 g/cm^3. The density and diameter of the cylindrical booster pellets were 1.68 g/cm^3 and 29.58 mm respectively. The new booster pellet (a) is shown in Figure 7. A cylindrical booster pellet is shown in Figure 8.

Figure 7. The new booster pellet (a).

Figure 8. A cylindrical booster pellet.

(2) Selection of the detonation explosive

RDX was used as the detonation explosive. The pressed-explosive density was 1.27 g/cm^3.

(3) Selection of the main charge explosive

A nitroguanidine (NQ)-based composite explosive and TNT were chosen as the main charge explosives. The density, diameter and height of the NQ-based composite explosive were 1.30 g/cm^3, 50.0 and 36.5 mm respectively, and those of TNT were 1.51 g/cm^3, 50.0 and 22.0 mm respectively.

(4) Selection of the steel witness plate

The steel witness plate was of general carbon steel size Φ 100×50 mm.

3.3 Experimental devices

The experimental device used to measure the initiation capacity is shown in Figure 9. The testing instrument for convergence pressure is illustrated in Figure 10.

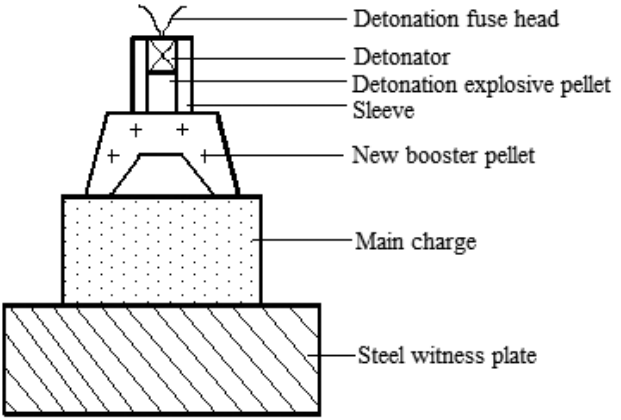

Figure 9. Experimental device of the main charge axial-steel-dent method.

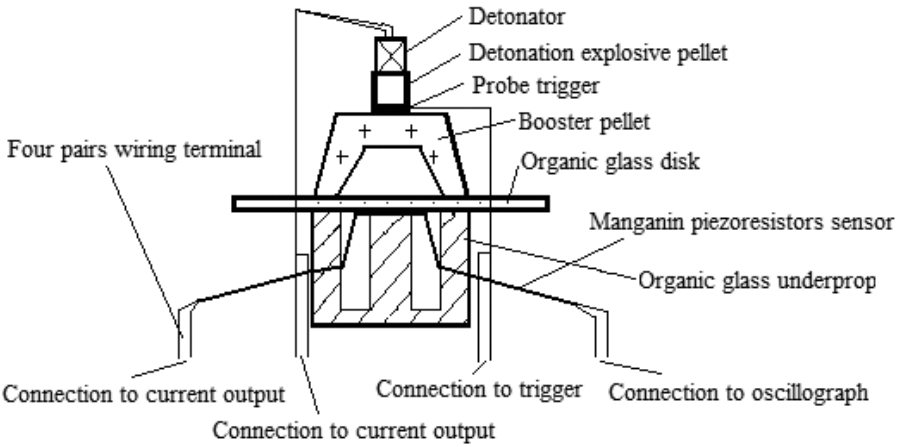

Figure 10. Diagrammatic illustration of the pressure test method.

3.4 Experimental results and discussion

3.4.1 Comparison of initiation capacities between the new booster pellet (a) and a cylindrical booster pellet

The initiation capacities of the new booster pellet (a) and a cylindrical booster pellet were measured using the main charge varied-composition method. The main charge explosive was an NQ-based composite explosive. The compositions were NQ, graphite and polytetrafluoroethylene (PTFE). The results are shown in Table 2.

Table 2. Results of the initiation capacities of the booster pellets by the varied-composition method

Main charge			Booster pellet		Initiation rate
NQ/PTFE/ Graphite	Mass (g)	Density (g/cm^3)	Shape	Mass (g)	
40/59/1	93.1	1.30	pellet (a)	19.35	0/5
			cylindrical	27.32	0/5
43/56/1	93.1	1.30	pellet (a)	19.35	5/5
			cylindrical	27.3	0/5
51/48/1	93.1	1.30	pellet (a)	19.35	5/5
			cylindrical	27.3	5/5

Table 2 shows that when the compositions of the main charge were NQ/PTFE/G=43/56/1, the initiation rate of the 19.35 g booster pellet (a) was 5/5. However, the initiation rate of a 27.3 g cylindrical booster pellet was 0/5. Therefore, the new booster pellet (a) has more initiation capacity than a cylindrical booster pellet with the same mass and pressed density.

3.4.2 Further study of the initiation capacity of the new booster pellet (a)
In these experiments, the main charge axial-steel-dent, the booster pellet axial-steel-dent, and the pressure test methods were used. The main charge was TNT. The results are shown in Table 3. Photos of the steel witness plates after the booster pellet axial-steel-dent method are shown in Figure 11.

Table 3. Results of the initiation capacities by the axial-steel-dent method and the pressure test method

Shape	Mass (g)	Dent data of method (2) (mm)	Dent data of method (3) (mm)	Convergence pressure (Gpa)
Cylindrical	19.7	2.80	2.65	26
Cylindrical	22.4	3.10	3.02	26
Cylindrical	26.7	3.28	3.44	26
Cylindrical	33.1	3.56	3.86	26
Pellet (a)	19.4	4.76	12.56	34

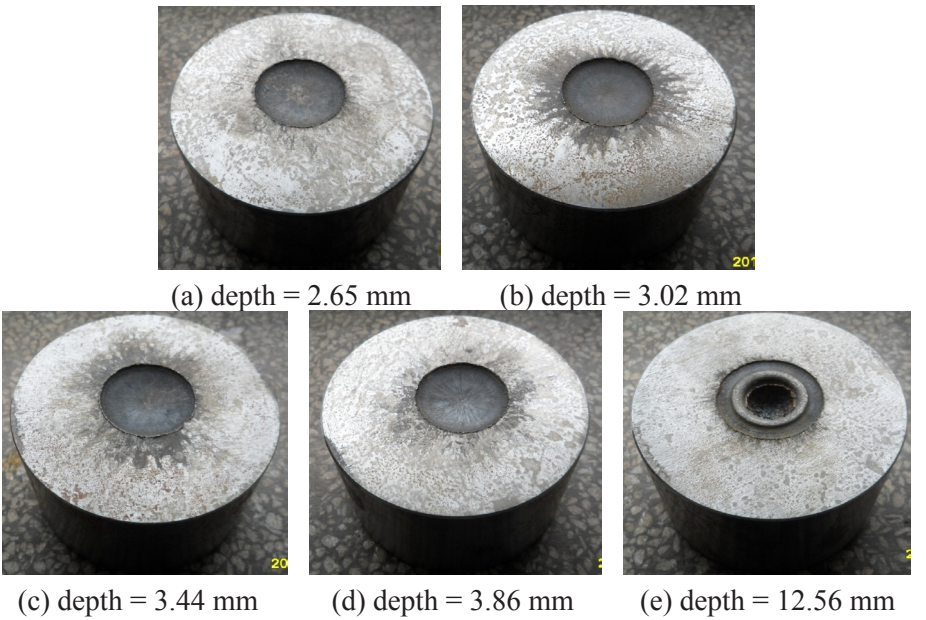

(a) depth = 2.65 mm (b) depth = 3.02 mm

(c) depth = 3.44 mm (d) depth = 3.86 mm (e) depth = 12.56 mm

Figure 11. Steel witness plates from the booster pellet axial-steel-dent method.

The steel dent depth of the new booster pellet (a) was larger than that of any cylindrical booster pellet for both the main charge and the booster axial-steel-dent methods. The convergence pressure of the new booster pellet (a) was 34 Gpa, larger than that of the cylindrical booster pellet (26 Gpa). The three test methods were in good agreement with each other.

In Figure 11(e), the hole in the centre is deep and the ring around the hole is shallow. The central hole is produced by the convergence pressure and the ring dent is produced by the detonation wave pressure. It also shows that the convergence pressure is larger than the detonation wave pressure.

4 Conclusions

The initiation capacities of two booster pellets were studied by numerical simulation and experiment. Several conclusions have been made:

- The initiation capacity of the new booster pellet is much better than that of the cylindrical booster pellet with the same mass and density.
- The convergence pressure of the new booster pellet was measured

experimentally for the first time. The convergence pressure of the new booster pellet was much higher than that of a cylindrical booster pellet with the same density.

- The various test methods were in good agreement with each other.

5 References

[1] *Department of Defense Test Method Standard: Hazard Assessment Tests for Non-Nuclear Munitions*, MIL-STD-2105B, Department of Defense, **1994**.

[2] Flegg G.T., Frankl P.J., Griffiths T.T., *Explosive Train Scale Shock Testing of New Energetic Materials*, QinetiQ, Fort Halstead, Sevenoaks, Kent, TN14 7BP, UK, **2010**.

[3] Spahn P.F., *Booster Explosive Ring*, US Patent 5233929, **1993**.

[4] Spahn P.F., *Embedded Can Booster*, US Patent 5221810, **1993**.

[5] Dallman J.C., *Measurements of Detonation-Wave Spreading and Local Particle Velocity at the Surface of 17-mm LX-07 Hemispherical Boosters*, Report No. LA-11414-MS, Los Alamos National Laboratory, **1988**.

[6] Hu L.S., Hu S.Q., Cao X., Study on the Initiation Capacities of Two Booster Pellets, *Cent. Eur. J. Ener. Mater.*, **2012**, *9*, 261-272.

[7] Lee E.L., Hornig H.C., Kury J.W., *Adiabatic Expansion of High Explosive Detonation Products*, Report No. UCRL-50422, Lawrence Livermore National Laboratory, Livermore, CA, **1968**.

[8] Alia A., Souli M., High Explosive Simulation Using Multi-Material Formulations, *Applied Thermal Engineering*, **2006**, *26*, 1032-1042.

[9] Johnson G.R., Cook W.H., Fracture Characteristics of Three Metals Subjected to Various Strains, Strain Rates, Temperatures and Pressures, *Eng. Fract. Mech.*, **1985**, *21*, 31-48.

[10] Li Y., *Experiment of Booster Shock Initiation and Its Numerical Simulation* (in Chinese), North University of China, China, **2010**.

[11] Foan G.C., Coley G.D., Shock Initiation in Gap Test Configuration, *7th Int. Symposium on Detonation*, Acr-221, Office of Naval Research, Arlington, VA, **1976**.

[12] Cao X., *Study on the Structure of High-Effect-Booster Charge and Numerical Simulation on Its Initiation Process* (in Chinese), North University of China, China, **2005**.